

MASS CONSERVATIVE COUPLING OF NON-HYDROSTATIC METEOROLOGICAL MODELS WITH AIR QUALITY MODELS

M. Talat Odman and Armistead G. Russell

School of Civil and Environmental Engineering
Georgia Institute of Technology
Atlanta, Georgia 30332-0512, USA

INTRODUCTION

The high-resolution data produced by recent non-hydrostatic meteorological models (MMs) are expected to significantly improve the characterization of transport in air quality models (AQMs). The study of the formation of secondary pollutants should greatly benefit from this improvement. However, the use of data from non-hydrostatic MMs presents new problems to the air quality modeler. First, there is the *consistency* issue. The wind components together with air density satisfy the continuity equation in MMs. On the other hand, AQMs rely on the species continuity equation to enforce the principle of mass conservation. Though the continuity equation does not appear explicitly in their formulation, AQMs are expected to maintain a uniform mass mixing ratio field for an inert tracer after transport with the winds produced by the MM. This expectation could only realize if the two models used the same *discretization*, i.e., grid, time step, and finite difference forms. However, the models may not share the same grid structure and the forms used for advection in AQMs are usually very different from those in MMs. Also, since the outputs of the MM are stored less frequently than the AQM time step, the input variables cannot be reconstructed exactly at the desired instants. Consequently, the winds and the air density used in AQMs may not be consistent (i.e., they do not satisfy the continuity equation) and the uniform tracer field cannot be maintained. The perturbation of uniform fields is usually more pronounced with data from non-hydrostatic MMs than with data from hydrostatic MMs for the same domains. These perturbations grow in time and may generate instabilities in AQM solutions. A second issue, species or tracer *mass conservation*, presents itself because of the attempts to establish consistency and produce stable results. In some existing AQMs, the conservation of species mass was sacrificed in order to obtain stable results. However, large mass conservation errors are not tolerable in AQMs used to establish source-

receptor relationships for the design of emission control strategies. Therefore, it is desirable to establish consistency in a mass-conservative manner.

METHODOLOGY

The use of data from non-hydrostatic models may lead to unstable solutions due to the consistency problem, as described above. Some widely used AQMs adopted an approach where a uniform tracer is transported along with other species and the concentrations are renormalized using the deviation of the tracer from uniformity as the norm. As a result the uniform mixing ratio field is maintained. However, the approach overlooks that non-linear advection schemes are used in AQMs for high accuracy. These schemes would affect fields of different distributions differently. Most species of interest, especially the emitted ones, have spatial distributions far from being uniform. Therefore, renormalizing the concentration of a species based on the perturbation of a uniform field can increase or decrease its mass artificially. We found that the mass conservation errors introduced by this approach are very large. Here, we will refer to this approach as “the flawed method.”

Species mass conservation is not sacrificed if the consistency of meteorological fields is established through the continuity equation. To satisfy the discrete continuity equation in the AQMs, wind or density fields (or both) from MMs must be adjusted. Lu et al. (1997) prefer adjusting the density field. Here we will describe three methods: two adjust the vertical wind component and a third adjusts the vertical flux. The methods also differ in the type of vertical advection algorithm used and whether a direct or iterative technique is used to solve for vertical wind component.

Method 1: Inverse Donor Cell

This method requires advection of air in addition to all the species and the use of the donor cell scheme for vertical advection.

$$c_k^{n+1} = c_k^* - \frac{\Delta t}{\Delta z_k} (w_{k+1/2} c_k^* - w_{k-1/2} c_{k-1}^*) \quad (1)$$

First, we apply horizontal wind components to the air density field, \mathbf{r}^n , to obtain an intermediate field \mathbf{r}^* . Any scheme can be used for horizontal advection; we used Bott’s scheme (Bott, 1989). Then, we require that the density after the vertical advection operator is applied to \mathbf{r}^* , be equal to \mathbf{r}^{n+1} . The latter is calculated from the MM data by using linear interpolation in time. Thus, we need to calculate a new value for vertical velocity that would yield the desired value of density. Substituting concentrations with air densities, Equation (1) is solved for $w_{k+1/2}$ as

$$w_{k+1/2} = \frac{1}{\mathbf{r}_k^*} \left(\frac{\Delta z_k}{\Delta t} (\mathbf{r}_k^* - \mathbf{r}_k^{n+1}) + w_{k-1/2} \mathbf{r}_{k-1}^* \right) \quad (2)$$

Since $w_{1/2} = 0$, Equation (2) can be used starting from the surface layer ($k=1$) and moving to the top, each time using the vertical velocity computed for the previous layer. The winds at the top of the model will usually have a vertical component. The vertical velocities computed from Equation (2) must be used in Equation (1) to advect all other pollutant species. Note that the horizontal advection operator must always be applied before the vertical. Also, since the donor cell scheme is subject to the Courant stability condition, the case when the Courant

number exceeds unity requires special treatment. Finally, the linear donor cell scheme is only first-order accurate.

Method 2: Inverse Bott Scheme

This method is very similar to Method 1 except a higher-order vertical advection scheme is used. Higher-order schemes are nonlinear because of the filters or flux limiters they use to eliminate the oscillations in the solution. Their non-linearity makes it difficult to solve for the vertical velocity field that would yield the air density \mathbf{r}^{n+1} when applied to the horizontally advected air density field \mathbf{r}^* . While a direct solution is not possible, iterative techniques can be used as suggested by Flatoy (1993). Here we used Bott's scheme with variable grid spacing for vertical advection. This scheme uses second-order area-preserving polynomials to represent the sub-grid distribution of concentration. The vertical velocity field can be calculated using the secant iteration technique.

$$w_{k+1/2}^{i+1} = w_{k+1/2}^i - \frac{w_{k+1/2}^i - w_{k+1/2}^{i-1}}{\mathbf{r}_k^i - \mathbf{r}_k^{i-1}} (\mathbf{r}_k^i - \mathbf{r}_k^{n+1}) \quad (3)$$

where \mathbf{r}_k^i denotes the density field that the Bott's scheme would produce under the wind field $w_{k+1/2}^i$. To start the iterations two initial guess are needed, $w_{k+1/2}^0$ and $w_{k+1/2}^1$. The wind calculated by inverting the donor-cell scheme serves as $w_{k+1/2}^1$. The other initial guess is taken to be 90% of $w_{k+1/2}^1$. We interpreted convergence as \mathbf{r}_k^i approaching \mathbf{r}_k^{n+1} by a certain tolerance. Note that a uniform mixing ratio field advected with this method would be subject to very small perturbations, which can be reduced by decreasing the tolerance. We found that a value of 0.5% is quite effective as a tolerance; smaller values led to unreasonably large number of iterations without too much improvement in the result.

Method 3: Inverse Donor Cell in 3-D and Russell and Lerner Scheme

This method is based on the approach described by Russell and Lerner (1981) and later used by Easter (1993). First the continuity equation is discretized in the following flux form.

$$\begin{aligned} \mathbf{r}_{i,j,k}^{n+1} = & \mathbf{r}_{i,j,k}^n - \frac{\Delta t}{\Delta x} (F_{i+1/2,j,k}^n - F_{i-1/2,j,k}^n) \\ & - \frac{\Delta t}{\Delta y} (G_{i,j+1/2,k}^n - G_{i,j-1/2,k}^n) - \frac{\Delta t}{\Delta z} (H_{i,j,k+1/2}^n - H_{i,j,k-1/2}^n) \end{aligned} \quad (4)$$

F, G, H are advective fluxes of air along the x, y, z directions, respectively. Then the species continuity equation is also written in the flux form.

$$\begin{aligned} c_{i,j,k}^{n+1} = & c_{i,j,k}^n - \frac{\Delta t}{\Delta x} (A_{i+1/2,j,k}^n - A_{i-1/2,j,k}^n) \\ & - \frac{\Delta t}{\Delta y} (B_{i,j+1/2,k}^n - B_{i,j-1/2,k}^n) - \frac{\Delta t}{\Delta z} (C_{i,j,k+1/2}^n - C_{i,j,k-1/2}^n) \end{aligned} \quad (5)$$

For consistency, the fluxes A, B, C must be related to their counterparts in Equation (4) by

$$A = Fr_x; B = Gr_y; C = Hr_z \quad (6)$$

where r_x, r_y, r_z are the average mixing ratios (i.e., c/\mathbf{r}) crossing the grid cell boundaries in the x, y, z directions, respectively. We defined F and G as donor cell fluxes and solved Equation (4) for the vertical flux $H_{i,j,k+1/2}^n$ much like the solution for $w_{k+1/2}^i$ in Method 1. For comparison to other methods, we derived the corresponding vertical velocity by interpreting H also as a donor cell flux. The use of first-order accurate donor cell scheme for horizontal advection of air should not introduce large errors since the air density fields do not have the large gradients found in pollutant fields. It is more important to use higher-order schemes for advection of pollutant species. We used Bott's fourth-order area-preserving polynomials in the horizontal and his scheme for variable grid spacing in the vertical to compute the mixing ratios r_x, r_y, r_z .

RESULTS AND DISCUSSION

Using the methods described above in an AQM (Odman and Ingram, 1996), we simulated a tracer experiment conducted during the Central California Air Quality Study (SARMAP). In this experiment inert tracers were released from different locations in the San Francisco Bay area and the Central Valley. All releases started at 6:00 PDT (Pacific Daylight savings Time) on August 3, 1990 and lasted for 3-4 hours. The release rates were approximately uniform. Starting two hours before the releases and using fields generated by the NCAR Meteorological Model (MM5) we ran the model for 48 hours. The AQM grid covered the SARMAP domain with 32x39 cells of 12 km size. In the vertical, the grid extended to the stratosphere with 15 non-uniformly spaced layers starting with a thickness of 60 m at the surface and increasing upward. During the simulation, we did not only follow the tracer concentrations but the adjustments to the vertical wind components as well. When we analyzed these adjustments, we found a strong correlation with the terrain height. The adjustments were largest over the slopes of the coastal range and the Sierra Nevadas.

We found insignificantly small differences among the vertical velocities generated by the three methods. Therefore we will only use the velocity from Method 1 in our comparisons with the vertical wind components provided by MM5. The averages and the standard deviations of the MM5 and adjusted vertical wind components as well as their difference are illustrated in Figure 1 for the surface layer. The adjustment reduces the magnitude of the vertical wind by about 25% during the day when there is an upward component with an average of about 0.03 m/s and by 35% at night when the vertical velocity is downward. The standard deviations are also reduced. The standard deviations are smallest early in the morning and largest in the afternoon and remain so up to about level 11 where we reach the free troposphere.

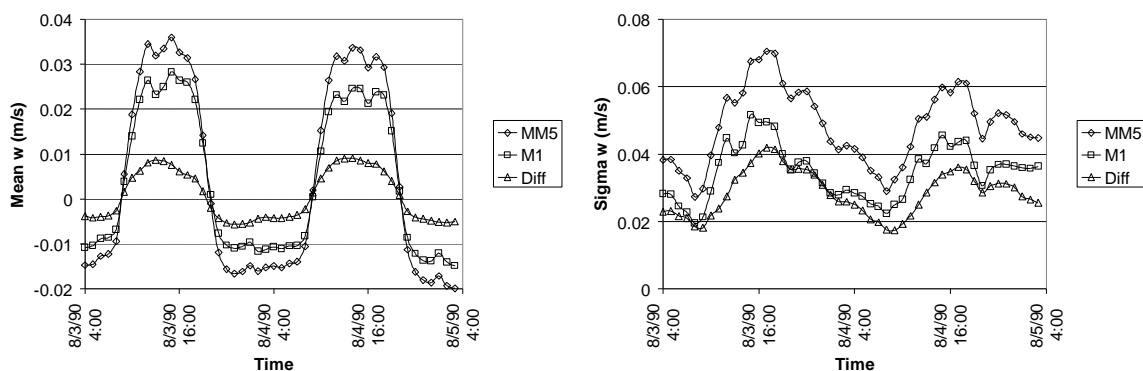


Figure 1. Time series of the mean (left) and standard deviation (right) of the first layer vertical velocity.

Table 1. Mean and standard deviation of vertical wind components in m/s.

Time	Layer	MM5		Adjusted ¹		Difference ²	
		Mean	σ	Mean	σ	Mean	σ
700	1	-1.22E-02	3.29E-02	-8.55E-03	2.28E-02	-3.65E-03	2.10E-02
	5	1.25E-02	3.65E-02	9.06E-03	3.83E-02	3.42E-03	3.12E-02
	11	1.08E-02	1.01E-01	1.40E-02	1.23E-01	-3.19E-03	8.50E-02
1500	1	3.59E-02	6.75E-02	2.83E-02	5.17E-02	7.63E-03	3.74E-02
	5	3.26E-02	1.13E-01	3.00E-02	1.03E-01	2.60E-03	5.88E-02
	11	4.27E-03	1.69E-01	3.39E-02	2.26E-01	-2.96E-02	1.64E-01

¹Method 1 is used to adjust the vertical velocity.

²The mean and standard deviation of the (MM5 - Adjusted) field.

The averages and standard deviations are given in Table 1 for three different layers, the surface (0-60 m), the 5th (386-513 m) and the 11th layers (2155-3570 m). The values are reported at 700 PDT and 1500 PDT on August 3, 1990. In the PBL, relative to the magnitude of vertical velocity, the magnitude of the adjustment decreases with altitude. While the afternoon average adjustment is 21% at the surface it is only 8 % in the 5th layer. The relative difference starts increasing upon reaching the free troposphere. This may be related to the fact that the vertical velocity is small aloft and that the layer thicknesses are increasing with height. Also MM5 sets the vertical velocity to zero at the top of the troposphere while there is no such condition with the adjusted velocity. Data for the second day of the simulation had similar trends. The adjustment to the vertical velocity may be large in certain locations, especially over sloping terrain, but even then the absolute value of the vertical wind is small enough (few tenths of 1 m/s) that we do not expect to see a large impact on tracer or pollutant transport.

The total mass of two tracers, PMCH and PMCP, as predicted by different methods is shown in Figure 2. The results of a simulation with unadjusted wind fields is also shown. The largest conservation error is associated with PMCH mass. This tracer was released from San Jose and has a trajectory over complex coastal terrain. While only 19 kg of tracer was released, the flawed method leads to an estimate of 46 kg of PMCH at 1100 PDT. Other methods are able to maintain total tracer mass at 19 kg as long as the tracer remains within the domain. The decrease in total mass after 2100 PDT is associated with tracer crossing the lateral or top domain boundaries. The mass conservation error of the flawed method is also significant (approximately 25 %) for the PMCP tracer released from Pittsburgh in the San Francisco Bay area. The error is not as significant for other releases from the Central Valley.

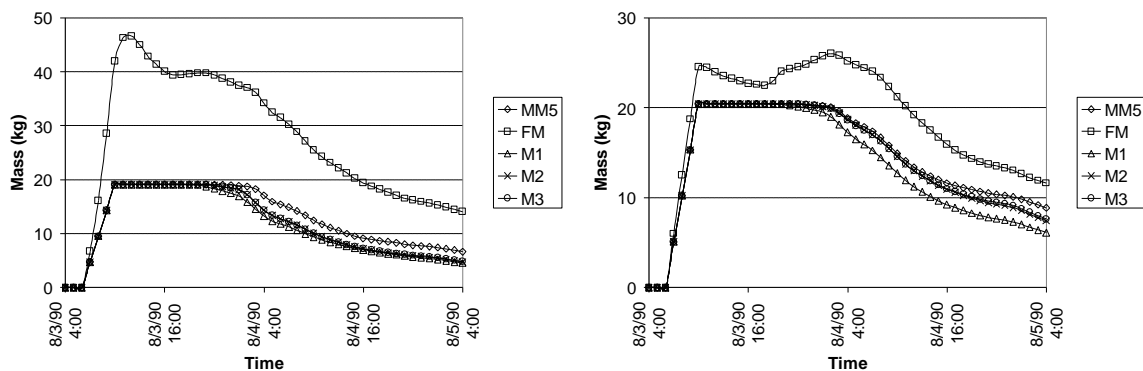


Figure 2. Time series of total mass of PMCH (left) and PMCP (right) as predicted by different methods: non-adjusted wind fields (MM5), flawed method (FM), and mass conservative Methods 1-3 (M1, M2, M3).

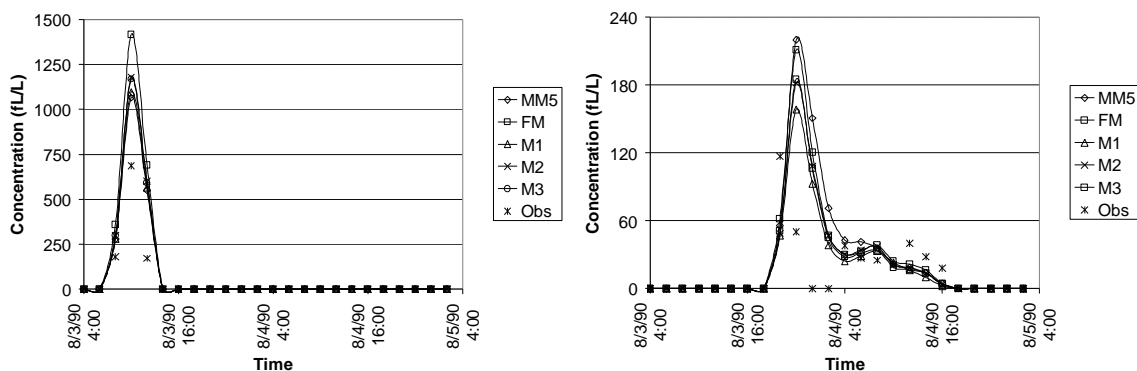


Figure 3. The time series of observed and predicted PMCP concentrations at Brentwood (left) and Friant (right).

In Figure 3 the time series of observed and predicted PMCP concentrations are shown at two sites. The distance from the release point to these sites, Brentwood and Friant, are approximately 30 and 220 km, respectively. The observations are provided as 2-hour averaged concentrations. The predicted concentrations were also averaged to match observations. The peak concentration predicted by all methods are larger than the observed peak at Brentwood. Compared to the flawed method, all three mass conservative methods yield a peak value closer to the observation, but the overprediction is still of the order of 60-70%. The closest value to the observation is obtained when MM5 winds are used without any adjustment. The predictions of the flawed method are not too far off from those of mass conservative methods. This indicates that the mass conservation errors are small along the trajectory to this site. At Friant the predicted peaks are closer to the observations but they display a time lag. This is not surprising given the relatively larger distance of this site from the release point. In contrast to the former site, the use of unadjusted MM5 winds led to the largest overprediction. The peak predicted by Method 1 is the closest to the observation. At both sites the difference between observed and predicted concentrations are larger than the differences between different methods. Therefore, it is difficult to judge which method performs better in this tracer transport simulation.

Using the same model settings a five-day ozone episode (August 2-6, 1990) was simulated over the same domain. The ground level ozone concentrations at 1700 PDT on August 5 are shown in Figure 4. The inconsistencies in MM5 wind fields led to instabilities during this simulation and yielded unreasonably high ozone. Methods 2 and 3 produced practically identical results therefore only Method 2 will be discussed. The differences between ozone levels predicted by the flawed method and Method 1 are of the order of 15 ppb near the coastal range. Method 1 predicts higher ozone concentrations in major source areas to the south of the San Francisco Bay, such as San Jose. On the other hand, further to the southeast (downwind), ozone concentrations predicted by Method 1 are lower. This may be due to an erroneous increase in the mass of nitrogen oxides in the flawed method. In comparison to Method 1, Method 2 predicted slightly higher (of the order of few ppb) ozone concentrations over the Central Valley and slightly lower concentrations over more complex terrain such as the coastal range and the foot-hills of the Sierra Nevadas. The maximum difference was observed at Fresno where Method 2 predicted 7 ppb higher ozone than Method 1. Recall that the differences between the vertical wind components of Method 1 and Method 2 were negligible. Therefore, the differences in ozone levels characterize the impact of using a more accurate vertical advection scheme in Method 2. Finally, the differences were more pronounced at night and early in the morning. For example at 900 PDT August 5, Method 1 predicted ozone levels 15 ppb lower than the flawed method at Sacramento and 25 ppb lower southwest of the Central Valley.

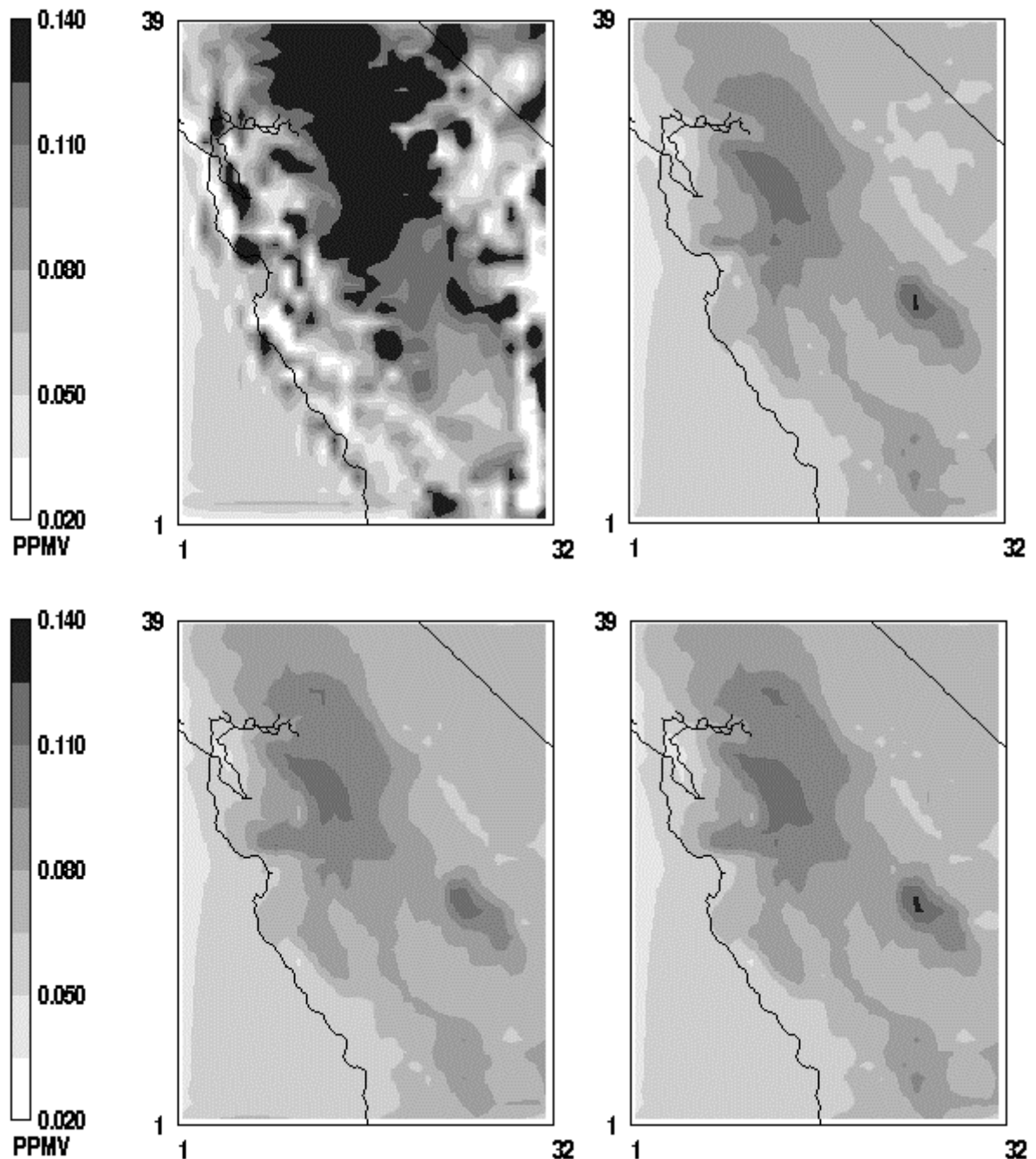


Figure 4. Spatial distribution of surface layer ozone at 1700 PDT August 5, 1990 as predicted by the non-adjusted wind fields (upper-left), flawed method (upper-right), and Methods 1 and 2 (lower left and right).

Figure 5 shows the maximum and the standard deviation of ground level ozone concentrations as predicted by different methods. On the first day, the flawed method predicts about 10 ppb lower peak ozone than the mass conservative methods. It also estimates a maximum concentration of 125 ppb at 900 PDT on August 5. This is about 45 ppb higher than the estimates of other methods. The peak ozone predictions of the flawed method are 10 to 20 ppb higher at night. Method 1 led to the lowest nighttime ozone estimates, with differences of up to 10 ppb from other methods early in the morning. The estimates of Methods 2 and 3 are almost identical. Method 1 resulted in the smallest standard deviation: as much as 1 ppb lower than other methods during the day and 1 to 2 ppb lower than Methods 2 and 3 at night. The nighttime standard deviation of the flawed method was the highest, about 2 to 4 ppb higher than Method 1.

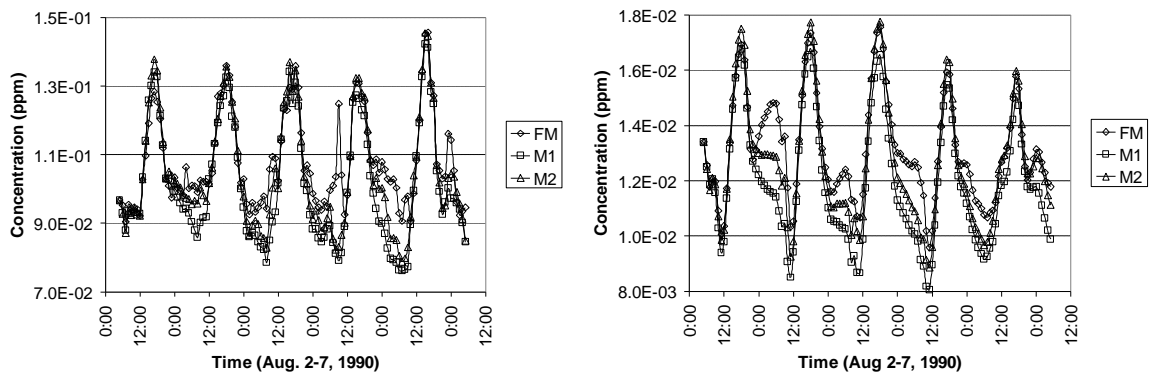


Figure 5. The time series of the maximum ozone concentration (left) and the standard deviation of surface layer ozone (right) as predicted by the flawed method (FM), and mass conservative Methods 1&2 (M1, M2).

CONCLUSIONS

The inconsistency of data from non-hydrostatic MMs may lead to instabilities in AQMs. Meteorological data can be made consistent without sacrificing the mass conservation characteristics of the AQM. Adjusting the vertical wind component proved to be an effective technique. We implemented and compared three methods for obtaining the vertical wind component from the discrete continuity equation. The methods differ in their vertical advection schemes. We found that the methods produced very similar vertical wind fields but these fields differed from those supplied by the MM. The adjustments reduced the vertical wind speed by an average of about 30% near the surface. The reduction was more pronounced at night when the winds have a weaker downward component. Also, the reduction decreased with altitude in the PBL but started increasing again in the free troposphere where the winds are practically horizontal. Thus, the adjustments may be large relative to the vertical winds but this is generally the case when the wind speeds are small. This implies that overall tracer transport would not be significantly affected by the adjustments. The tracer experiment simulation provided partial support for this hypothesis. Along a limited number of trajectories the original and adjusted wind fields yielded similar results. Unfortunately, the uncertainties in the tracer data and other parameters of the AQM are too large for more definite conclusions. We were unable to determine which one of the three methods best characterizes tracer transport. In an air quality simulation there were small differences in ozone levels predicted by the three methods. These are due to the use of vertical advection schemes of different accuracies. Methods with higher-order schemes seem to perform better but a more complete evaluation is needed at this point.

References

- Bott, A., 1989, A positive definite advection scheme obtained by nonlinear renormalization of the advective fluxes, *Mon. Wea. Rev.* 117:1006.
- Easter, R.C., 1993, Two modified versions of Bott's positive-definite numerical advection scheme, *Mon. Wea. Rev.* 121:297.
- Flatoy, F., 1993, Balanced wind in advanced advection schemes when species with long lifetimes are transported, *Atmos. Environ.* 27A:1809.
- Lu, R., Turco, R.P., and Jacobson, M.Z., 1997, An integrated air pollution modeling system for urban and regional scales: 1. Structure and performance, *J. Geophys. Res.* 102:6063.
- Odman, M.T, Ingram, C., 1996, Multiscale Air Quality Simulation Platform (MAQSIP): Source Code Documentation and Validation, MCNC Technical Report ENV-96TR002, Research Triangle Park, North Carolina.
- Russell, G.L., and Lerner, J.A., 1981, A new finite-differencing scheme for the tracer equation, *J. Appl. Meteor.* 20:1483.